



## طراحی و مشخصه‌یابی یک مدولاتور فاز سیلیکونی جدید مبتنی بر ساختار تخلیه حامل جانبی

محمد صادق میرزایی، حمید رضا مشایخی، محمد حسین زندی

دانشکده فیزیک، دانشگاه شهید باهنر، کرمان، ایران

چکیده- در این مقاله، از طریق شبیه سازی‌های الکتریکی و نوری، یک مدولاتور فاز سیلیکونی تخلیه حامل فشرده در طول موج  $1.3\mu\text{m}$  ارائه می‌شود. شیفتهنده فاز، متشکل از یک پیوند PN جانبی بایاس معکوس با طول  $120\mu\text{m}$  است. با طراحی دقیق پیوند PN، بازده مدولاسیون محاسبه شده، مقادیر بین  $1/0.2$  و  $2/27\text{cm}$  را در بر می‌گیرد. اتلاف نوری این شیفتهنده فاز فشرده در  $4\text{V}$  برابر  $2/49\text{dB/cm}$  است. همچنین این ساختار عملکرد سرعت بالا  $30\text{GHz}$  را فراهم می‌کند. بهبود بیشتر در عملکرد آن در مقایسه با شیفتهنده‌های فاز پیشین، حاصل می‌شود.

کلید واژه- فوتونیک سیلیکونی، مدولاسیون نوری، اثر تخلیه حامل، شیفتهنده فاز سیلیکونی

## Design and Characterization of a Novel Silicon Phase Modulator based on the Lateral Carrier Depletion Structure

Mohammad Sadegh Mirzaei, Hamid Reza Mashayekhi, and Mohammad Hossein Zandi

Department of physics, Shahid Bahonar University, Kerman, Iran

**Abstract-** In this paper, through electrical and optical simulations, a compact-sized carrier depletion silicon phase modulator operating in  $1.3\mu\text{m}$  is presented. The phase shifter is composed by a  $120\mu\text{m}$ -long reverse biased PN junction. With the precise design of the PN junction, the calculated modulation efficiency contains between  $1.02$  and  $2.2\text{V.cm}$ . The compact phase shifter optical loss is  $2.49\text{dB/cm}$  at  $4\text{V}$ . Also, this structure provides  $>30\text{GHz}$  high speed operation. Further improvement in its performance in comparison to the state of the art phase shifters is obtained.

Keywords: Silicon photonics, Optical modulation, Carrier depletion effect, Silicon phase shifter

## 1. Introduction

With the development of communication systems and optical interconnects, silicon photonics technology has drawn significant attention in recent years due to low cost, high performances and direct compatibility with complementary metal oxide semiconductor (CMOS) technology. Optical modulators are one of the silicon photonics building blocks which are used for optical data in optical interconnect [1]. Fast modulation in silicon can be obtained by plasma dispersion effect [2]. It is widely used from the carrier depletion mechanism for achieving high speed modulators. High modulation efficiency, small size, low optical loss and high bandwidth are some figures of merit of the modulators. A lot of work has been done in the field of carrier depletion based silicon optical modulators to improve its functionality [3-5]. However, further improvement in silicon modulators for telecommunication applications is desirable. In this paper, we have investigated the concept of the compact-sized low-loss phase shifter for a silicon modulator. We performed device simulation for the phase shifter using electrical and optical simulation environments [6] and observed a performance improvement in comparison with other structures.

## 2. Theory and simulation method

The schematic of phase shifter cross section is shown in Fig. 1. It is a rib waveguide with an embedded lateral PN junction based on the silicon on insulator (SOI) platform. The phase shifter length is  $120\mu\text{m}$  with  $250\text{nm}$ -thick top Si and  $1\mu\text{m}$ -thick buried oxide. The silicon rib waveguide has a width of  $400\text{nm}$ , a height of  $250\text{nm}$  and a slab thickness of  $80\text{nm}$ . The  $80\text{nm}$  slab thickness is chosen to maximize the optical mode confined in the rib waveguide core. Also, this thin slab gives electrical access to the junction. The P-type and N-type region are chosen to form a PN junction. The offset between PN junction and core of the rib waveguide is  $100\text{nm}$  towards the N region, because the holes provide a larger change in refractive index compared to electrons. Therefore, this makes

to optimize the modulation efficiency. The heavily doped regions ( $1\times 10^{20}$ ) connected to copper electrodes are chosen to ensure a good Ohmic contacts. In order to reduce the total loss, P++ and N++ regions are placed  $700\text{nm}$  away from the rib sides. By reducing the rib waveguide width to  $400\text{nm}$ , low optical loss and strong optical mode confinement is achieved. Here, there is a depletion region induced by the DC reverse bias voltage in the core of the rib waveguide. As the applied voltage increases, the depletion region becomes wider.

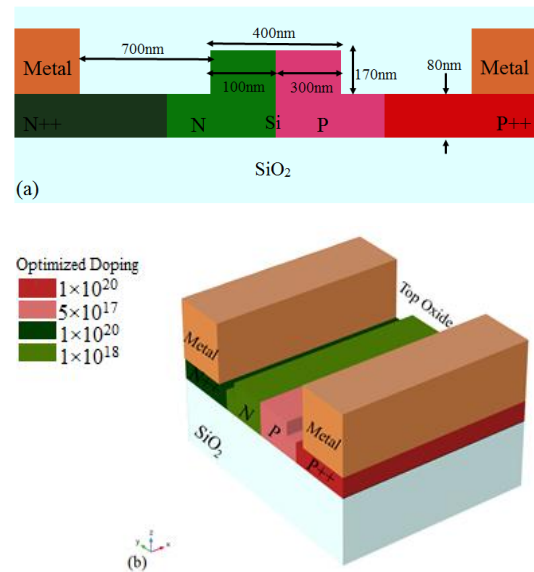


Fig. 1: (a) Schematic cross section of the lateral PN junction based optical phase shifter. (b) 3-D view of the phase shifter.

We use a device simulation package called Lumerical **DEVICE** to calculate its electrical characteristics. In the simulation, the Masetti's [7] model is applied and carrier statistics are assumed to be Fermi-Dirac. This simulator numerically solves the Poisson's equation and the charge continuity equation for electrons and holes. Its results include carrier distribution at different biases. An applied DC voltage was swept from 0 to 5V in device anode with 0.5V step. The carrier distribution is converted to the distribution of refractive index and absorption coefficient by carrier plasma relationship at  $1.3\mu\text{m}$  [2]. Finally, using of a finite difference mode solver, the effective index at different biases is calculated [6].

Therefore, with calculation of the effective index, it is easy to calculate optical phase modulation

$$\Delta\varphi = \frac{2\pi\Delta n_{eff}}{\lambda} \quad (1)$$

Where  $L$  is phase shifter length and  $\lambda$  is the wavelength of the light in vacuum, set as  $1.3\mu\text{m}$  in telecommunication systems. The modulation efficiency ( $V_{\pi}L$ ) defined as the applied voltage and length required to achieve a  $\pi$  phase shift can be directly calculated from the phase shift relationship (equation (1)). Moreover, the optical loss is obtained by the imaginary refractive index at different bias voltages.

### 3. Simulation results and discussion

In the phase shifter structure, the optimized doping concentrations are chosen to maximize the effective index change, but the optical loss does not increase. The waveguide dimensions have been optimized to maximize the optical mode confinement (as shown in Fig. 2). An optical mode profile is needed to show the fundamental mode propagating behaviour along the phase modulator. Fig. 2 indicates the optical profile showing that the most part of the light is confined in the phase shifter active area.

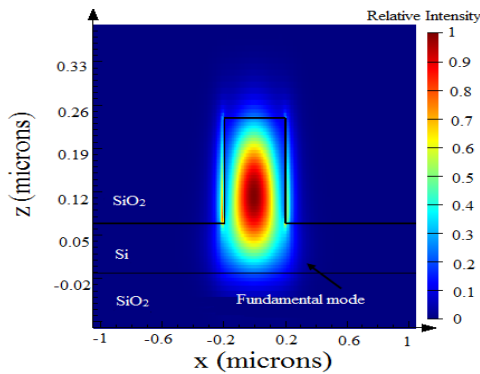


Fig. 2: Optical mode profile at  $1.3\mu\text{m}$ .

Fig. 3 shows the semiconductor region band diagram of the phase shifter which its depletion region width is  $310\text{nm}$ . However, the change in the effective index is dependent on the carrier concentration and the doping profile. The results of  $V_{\pi}L$  product as a function of applied reverse bias has been presented in Fig. 4.

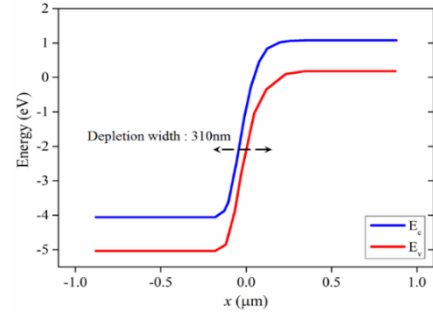


Fig. 3: Phase shifter semiconductor region band diagram in  $4\text{V}$  reverse bias voltage.

We saw that effective index change at  $4\text{V}$  reached about  $1 \times 10^{-4}$  (as shown in Fig. 4).

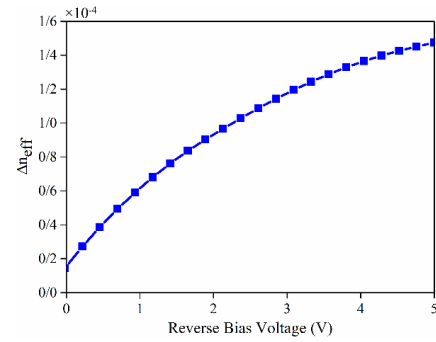


Fig. 4: Effective refractive index change as a function of the reverse bias voltage.

The phase shifter shows a modulation efficiency between  $1.02$  and  $2.2\text{V.cm}$  for a range of reverse bias voltage from  $1$  to  $5\text{V}$  (as illustrated in Fig. 5). We introduced a phase shifter figure of merit ( $V_{\pi}L\alpha$ ) where  $\alpha$  refers to the optical loss due to the free carrier absorption. For example, at  $4\text{V}$  its value reaches about  $\sim 4.8\text{V.dB}$  as shown in Fig. 5. Since modulator structures are usually long so low optical loss for the phase shifter is vital.

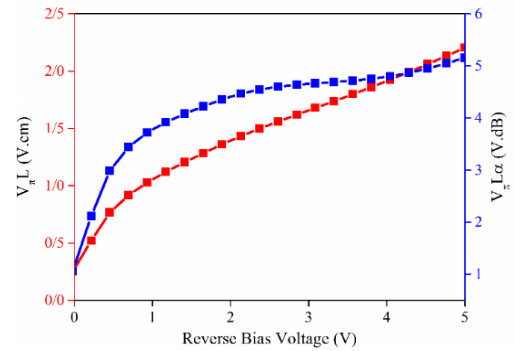


Fig. 5: The modulation efficiency and  $V_{\pi}L\alpha$  of the phase shifter under different reverse biases.

Fig. 6 shows optical loss  $\alpha$  as a function of the reverse bias voltage for 120 $\mu$ m phase shifter. The optical loss decreases by increase of the reverse bias voltage. The small signal electro-optic response of the 120 $\mu$ m phase shifter modulator under the reverse bias 0V, 2V and 5V was measured by using a network analyser. When the reverse bias is 5V, the 3dB bandwidth is approximately 38GHz (Fig. 7).

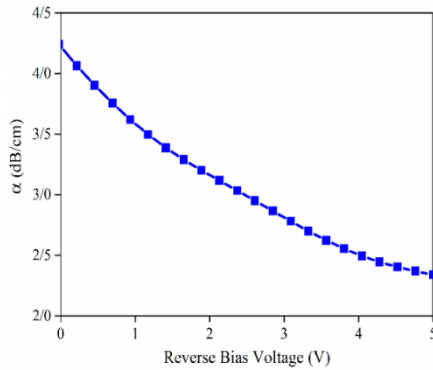


Fig. 6: The optical loss  $\alpha$  as a function of reverse bias voltage.

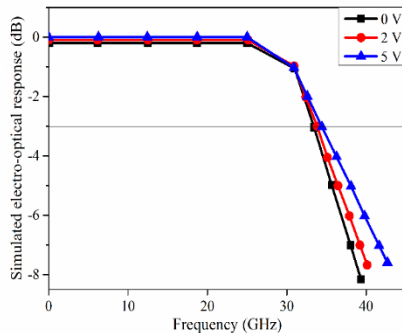


Fig. 7: Frequency response of a 120 $\mu$ m phase shifter modulator under different DC biases.

Table I shows a comparison of the performance with previously reported silicon phase shifters.

Table I. The comparison of between this work results with previous done works.

|           | Length ( $\mu$ m) | $V_{\pi}L$ (V.cm) | Optical loss(dB/cm) | EO bandwidth (GHz) |
|-----------|-------------------|-------------------|---------------------|--------------------|
| [8]       | 750               | 2.05              | 8.6                 | 28                 |
| [9]       | 500               | 1.8               | 3.1                 | 36                 |
| This work | 120               | 1.3               | 2.49                | 38                 |

#### 4. Conclusion

We have presented the design and simulation of a 120 $\mu$ m phase shifter based on lateral PN junction in a 250nm SOI platform. The presented phase shifter shows a modulation efficiency 1.02-2.2V.cm with an optical loss  $\alpha$  2.49dB/cm at 4V. This simulation results are in agreement with experimental results. This structure will be very useful in practical applications.

#### References

- [1] B. Jalali and S. Fathpour, "Silicon photonics," J. Lightwave Tech. vol. 24, pp. 4600–4615, 2006.
- [2] R.A. Soref and B.R. Bennett, "Electrooptical effects in silicon," IEEE J. Quantum Elec. vol. 23, pp. 123–129, 1987.
- [3] D. Pérez-Galacho, D. Marris-Morini, R. Stoffer, E. Cassan, C. Baudot, T. Korthorst, F. Boeuf, and L. Vivien, "Simplified modeling and optimization of silicon modulators based on free-carrier plasma dispersion effect," Opt. Express, vol. 24, pp. 26332–26337, 2016.
- [4] Wang, J., Qiu, C., Li, H., Ling, W., Le Li, Pang, A., Sheng, Z., Wu., and Gan, F., "Optimization and Demonstration of a Large-bandwidth Carrier-depletion Silicon Optical Modulator," J. Lightwave Tech., vol. 31, pp. 4119–4125, 2013.
- [5] Xu, H., Li, X., Xiao, X., Li, Z., Yu, Y., and Yu, J., "Demonstration and Characterization of High-Speed Silicon Depletion-Mode Mach-Zehnder Modulators," IEEE J. Select. Topics Quantum Electron. vol. 20, pp. 23–32, 2014.
- [6] L. Chrostowsky and M. E. Hochberg, *Silicon photonics design: from devices to systems*, Cambridge, pp. 28-46, 2015.
- [7] G. Masetti, M. Severi, and S. Solmi, "Modeling of Carrier Mobility against Carrier Concentration in Arsenic-, Phosphorus-, and Boron-Doped Silicon," IEEE Transactions on Electron Devices, vol. 30, No. 7, pp. 664-770, 1983.
- [8] Xiao, X., Xu, H., Li, X., Li, Z., Chu, T., Yu, Y., and Yu, J., "High-speed, low-loss silicon Mach-Zehnder modulators with doping optimization," Opt. Express, vol. 21, pp. 4116–4125, 2013.
- [9] Félix Rosa, M., Rathgeber, L., Elster, R., Hoppe, N., Föhn, T., Schmidt, M., and Berroth, M., "Design of a carrier-depletion Mach-Zehnder modulator in 250 nm silicon-on-insulator technology," Adv. Radio Sci. vol. 15, pp. 269-281, 2017.